Interactions of Polyaromatic Compounds I: Nanoaggregation Probed by Electrospray Ionization Mass Spectrometry and Molecular Dynamics Simulations

Journal:	*Energy & Fuels*
Manuscript ID	Draft
Manuscript Type:	Article
Date Submitted by the Author:	n/a
Complete List of Authors:	Liu, Lan; Univ of Alberta, Chemical & Material Engineering Xu, Zhenghe; University of Alberta, Chemical and Materials Engineering Zhang, Rongya; University of Alberta, Chemical and Materials Engineering Wang, Xi; University of Alberta, CME Simon, Sebastien; Norwegian University of Sciences and Technology Sjoblom, Johan ; Norwegian University of Science and Technology , Department of Chemical Engineering Jiang, Bin; Tianjin University, School of Chemical Engineering and Technology; Tianjin University, National Engineering Research Centre of Distillation Technology

Interactions of Polyaromatic Compounds I: Nanoaggregation Probed by Electrospray Ionization Mass Spectrometry and Molecular Dynamics Simulations

Lan Liu,[1†] Rongya Zhang,[1,2†] Xi Wang,[1] Sébastien Simon,[3] Johan Sjöblom,[3] Zhenghe Xu,[1] Bin Jiang[2]*

[1]Department of Chemical and Material Engineering, University of Alberta, Edmonton, Alberta, Canada T6G 1H9

[2]School of Chemical Engineering and Technology, Tianjin University, Tianjin 300072, China

[3]Ugelstad Laboratory, Norwegian University of Science and Technology, 7491 Trondheim, Norway

† Lan Liu and Rongya Zhang contributed equally to this work.

Abstract

Nanoaggregation of three synthetic polyaromatic compounds, N-(1-hexylhepyl)-N'-(5-carboxylicpentyl)-perylene-3, 4, 9, 10-tetracarboxilicbisimide (C5Pe), N-(1-undecyldodecyl)-N'-(5-carboxylicpentyl)-perylene-3,4,9,10-tetracarboxylbisimide (C5PeC11) and N,N'-bis(1-undecyldodecyl)perylene-3,4,9,10-tetracarboxylbisimide (BisAC11) individually or in their binary mixtures was studied under various solution conditions using electrospray ionization mass spectrometry (ESI-MS) and molecular dynamics (MD) simulation. The results from ESI-MS showed a significant enhancement in nanoaggregation of each individual component by increasing their concentration or heptane addition to toluene. Mixing a polyaromatic compound of longer aliphatic chain with a shorter chain polyaromatic compound in a given solvent was found to reduce the apparent average nanoaggregation number significantly. Replacing the -COOH group with an aliphatic group induced further steric hindrance to nanoaggregation of polyaromatic cores in the mixture. The results from MD simulations showed a similar trend of reducing nanoaggregation by mixing of two different polyaromatic compounds. The results of MD simulation further revealed that π-π stacking between polyaromatic cores is the major driving force for nanoaggregation while steric repulsion and strong solvation of longer aliphatic chains connected to the polyaromatic core hinder nanoaggregation of polyaromatic compounds studied. The results from this study provide a scientific basis for controlling nanoaggregation of polyaromatic compounds and shed lights on understanding the observed aggregation of asphaltenes in crude oil.

Introduction

The aggregation of hydrophobic surface active agents is an important topic both from fundamental and technical point of view. The progress in aggregation of polyaromatic compounds in organic solvent is quite different from that of hydrophilic surfactants in water. In water the surfactant molecules have an abrupt change from monomeric to aggregation state at a concentration that we call critical micelle concentration, cmc.[1-2] The driving force for such an aggregation is intrinsic to the structure of the molecules with distinct hydrophilic, polar or ionic and hydrophobic moieties. The difference in interaction energies between the hydrophilic and hydrocarbon moieties with water in the hydrophilic surfactant is so large that drives the aggregation of the hydrophilic surfactant molecules from monomers directly to large aggregates or known as micelles. In a hydrocarbon media the energy changes in relation to aggregation processes are minor, which leads to a slow and gradual progress in molecular aggregation of polyaromatic molecules in solvent.[3-5] In this case, the aggregation in the absence of water propagates via a stepwise pathway, normally remaining at a relatively low aggregation state. In this study we chose three different hydrophobic polyaromatic molecules of distinct and well-defined structures. These molecules capture all elements central for molecular aggregation in an organic medium. These elements are hydrogen bonding, π-π stacking and direct hydrophobic alkyl chain interaction. The molecular family represented in this paper could make a molecular system of well-defined polydispersity in structure and polarity. The aggregation found in this study encompasses early stage of molecular aggregation with only a few molecules involved (oligomers) to probe the buildup mechanisms of larger nanoaggregates that depends on the molecular structure, the concentration and the polydispersity.

During the last decade, various polyaromatic compounds have been synthesized and their aggregation in hydrocarbon media have been widely studied.[6-10] For instance, Akbarzadeh *et al.* synthesized pyrene-based compounds and studied their self-association.[6] Rakotondradany and coworkers synthesized and characterized hexabenzocoronene compounds using experimental methods and computational modeling. Later the properties of these synthesized asphaltene-type compounds were compared to with the properties of real asphaltenes under extraction and upgrading conditions.[6] Gray's group studied the self-association of pyrene derivatives of 2,2-bipyridine, which was attributed to π-π stacking between pyrene rings and bipyridine spacer.[7] Recently, Sjöblom's group designed a series of polyaromatic compounds of varied polar groups by incorporating a fixed hydrophobic part with a branched alkyl chain to a polyaromatic core (perylene).[9,10] This latest class of polyaromatic compounds is designed with a varying number of aromatic rings and molecular weights within the range of average asphaltene molecules in crude oil. The successful design and synthesis of this class of polyaromatic compounds opened the door for us to better understand the influence of heterogeneity and polydispersity in real asphaltenes systems on their nanoaggregation and flocculation. Extensive studies showed that the perylene-based polyaromatic compounds exhibit similar solubility and interfacial properties to real asphaltenes, which makes them a promising model compound to mimic central properties of asphaltene molecules in crude oil.[9,10] These polyaromatic compounds of well-defined molecular structures have been successfully used as model compound for molecular dynamics simulation to investigate their aggregation in solvent,[11,12] and adsorption at oil-water interfaces from the bulk oil phase.[13] It was found that variation in the structure of side chains and polarity of functional groups leads to significant variations in molecular association in bulk solvent and at oil-water interface.[11-13] The effect of aliphatic side-chain length on the aggregation of model asphaltenes

was also elucidated by Subir Bhattacharjee.[14] However, the reported experimental and computational studies have mainly focused on nanoaggregation and flocculation of single synthetic polyaromatic compounds, which cannot represent the real asphaltenes of complex polydispersity .

Perylene-based compounds can be easily mixed to represent different levels of polydispersity. In this study, we synthesized N-(1-hexylhepyl)-N'-(5-carboxylicpentyl)-perylene-3, 4, 9, 10-tetracarboxilicbisimide (C5Pe), N-(1-undecyldodecyl)-N'-(5-carboxylicpentyl)-perylene-3,4,9,10-tetracarboxylbisimide (C5PeC11) and N,N'-bis(1-undecyldodecyl)perylene-3,4,9,10-tetracarboxylbisimide (BisAC11) (Figure 1) as the model systems for this study. This family of polyaromatic compounds expresses polydispersity in terms of molecular weight, polarity and functionality, which allows us to probe the effect of polydispersity on molecular nanoaggregation of polyaromatic molecules. In this paper, we report the important findings obtained using electrospray ionization mass spectrometry (ESI-MS) and molecular dynamics (MD) simulation, probing key steps in nanoaggregation of well-defined polyaromatic compounds and their mixtures to better understand the problematic role of natural polyaromatic asphaltenes in oil production.

Materials and Methods

Samples and sample preparation

Three polyaromatic compounds, C5Pe (686.8 Da), C5PeC11 (827.1 Da) and BisAC11 (1035.6 Da) were synthesized in house by following the procedures described elsewhere (Figure 1).[9,10] All chemicals were purchased from Fisher Scientific (Ottawa, Canada) and used in the synthesis of these aromatic compounds without purification. Toluene (HPLC grade, 99.5%), methanol

(Optima LC-MS grade) and heptane (HPLC grade 99.5%) were used as solvents in all the experiments reported here.

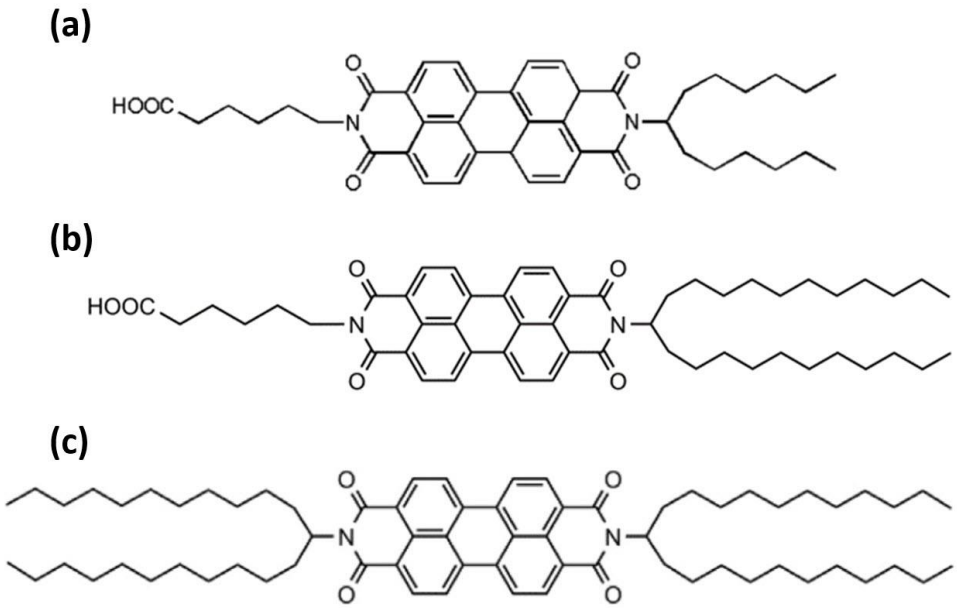

Figure 1. Structures of (a) C5Pe; (b) C5PeC11; and (c) BisAC11.

The stock solutions of polyaromatic compounds were prepared by dissolving a known mass of materials in toluene to yield a final concentration of 146~200 μM under sonication for 45 minutes for the use in ESI-MS measurements. A desired volume of ammonium acetate in methanol solution was added into the ESI solution to facilitate ionization of polyaromatic compounds.

Mass spectrometry (ESI-MS)

MS measurements were performed on a QTrap 4000 mass spectrometer (Applied Biosystems, Foster City, USA) equipped with a Turbo V^{TM} ion source. The solution sample was introduced into mass spectrometer by a syringe pump (Harvard Apparatus) at a flow rate of 7 µL/min. The mass spectrometer was operated in the negative ion mode with Q1 MS scan mode (m/z 100-2800

Da) at a rate of 1000 Da s^{-1}. The operating conditions of the mass spectrometer were set as follows: source temperature at 100 ^{o}C, curtain gas (CUR) at 10 L/min, ion spray (IS) at -4500 V, nebulizer gas (GS1) at 10 L/min, declustering potential (DP) at -10 V, entrance potential (EP) at -13 V and the cascade electron multiplier (CEM) at 2200 V with the interface heater ON. Data were collected and analysed by Analyst 1.6 software (Applied Biosystems). All the measurements were conducted at 25 ^{o}C, unless otherwise stated.

Molecular Dynamics Simulation

Simulation method and model

All the MD simulations were carried out using the GROMACS 5.1.2 software package. The GROMOS96 force field with the 53a6 parameter set was used in all the calculations reported here.[15-18] The initial coordinates of three polyaromatic compounds and toluene were drew and optimized using Material studio 8.0 software. Those structures were then transferred, as an input file, to the Automated Topology Builder (ATB) and Repository server (version 2.2) to generate the necessary molecular topology and GROMACS structure files.[19-21] All the double bonds and aromatic rings were modelled with sp^2 hybridized carbons. Furthermore, the polar and aromatic hydrogen atoms were modelled explicitly while aliphatic hydrogens were treated as unified interaction sites (united-atom model). Charges for polyaromatic compounds and toluene were adopted from Material studio geometry optimization. The molecular topology and GROMACS structure files for methanol were adopted from GROMACS. The sensitivity and applicability of GROMOS96 force field and simulation parameters described above to polyaromatic molecules have been validated previously for its successful application to studying nanoaggregation of polyaromatic molecules.[11,12,22,23] Furthermore, our computed values of the density, self-diffusivity, and enthalpy of toluene evaporation agree well with reported experimental results

(Supporting Information S1). Therefore, given a sufficiently long period of simulation time (~30 ns), we are confident that the force field and simulation conditions used in this study would reproduce reasonably well the experimental observations on aggregation of polyaromatic molecules at the specified temperature and pressure in our systems.

Simulation setup and conditions

Molecular dynamics simulation of five systems containing well-defined polyaromatic molecules in a methanol-toluene (M-T) mixture at 50:50 methanol:toluene volume ratio were performed over the time range of 30 ns. Initially, the dimension of the simulation box was set at 12 nm × 12 nm × 12 nm. A total of five simulation boxes were constructed as shown in Table 1. The polyaromatic molecules were initially randomly placed in the box. Pure polyaromatic molecules systems were simulated to study the effect of polyaromatic molecule's structure on aggregation. Mixtures of polyaromatic molecules were studied to investigate the polydispersity's effect on aggregation.

Table 1. Composition of polyaromatic molecules in toluene-methanol mixture systems.

System	Polyaromatic molecules	Time (ns)	Number of solvent molecules ($N_{methanol}$ + $N_{toluene}$)	Final volume (nm×nm×nm)
1	24 C5Pe	30	9605 + 3151	10.68×10.68×10.68
2	24 C5PeC11	30	9576 + 3118	10.68×10.68×10.68
3	24 BisAC11	30	9521 + 3099	10.69×10.69×10.69
4	24 C5Pe + 24 C5PeC11	30	9395 + 3023	10.65×10.65×10.65
5	24 BisAC11 + 24 C5PeC11	30	9288 + 2966	10.66×10.66×10.66

Each system was solvated with methanol-toluene mixture. After setting up the initial configuration, the system energy was minimized using the steepest descent method, followed by the conjugate gradient method as implemented in GROMACS 5.1.2. During energy

minimization, a cut-off distance of 1.2 nm was used for both Coulomb and van der Waals interactions. The system maximum energy was converged to less than 200 kJ mol^{-1} nm^{-1} threshold value to generate a stable system for the simulation. The detailed information on the simulated systems is listed in Table 1. All simulations were carried out under the NPT ensemble at 298 K and 1 bar pressure. For the first 3 ns, the Berendsen thermostat and Barostat were used to quickly relax the system to a constant pressure and temperature. After 3 ns, all the simulations were performed using Nose-Hoover thermostat[24] and Parrinello-Rahman pressure coupling algorithm.[25,26] The pressure and temperature coupling constants of τ_p = 3 ps and τ_T = 0.3 ps, respectively, were used throughout the simulations. In all the simulations, an isothermal compressibility of 9.08×10^{-5} bar^{-1} was applied. Periodic boundary condition (PBC) was applied in the x, y and z directions, and a leapfrog Verlet algorithm[27] with a time step of 2 fs was used for integration of the trajectories. The electrostatic interaction was computed using the particle-mesh Ewald summation (PME) method with a fast Fourier transform (FFT) grid spacing of 0.16 nm to account for long-range electrostatic interactions of the system. A 1.4 nm cut-off distance was used for the van der Waals interactions during MD production, which is consistent with GROMOS96 parameterization.[28] All bond lengths in our system were constrained using LINCS algorithm.[29] A neighbour list with a cut-off distance of 1.2 nm was updated every 5 steps. The initial atomic velocities of the system were set using the Maxwell-Boltzmann distribution employed in GROMACS at the specified temperature of 298 K. The structure and dynamic properties of the system after simulations were analysed using the GROMACS built-in analytical tools. The time evolution of the structure of the system was visualized using visual molecular dynamics (VMD).[30]

Results and Discussion

Nanoaggregation of synthetic polyaromatic compounds

ESI-MS has been widely used to detect and quantify the solution equilibria for various non-covalent donor-acceptor associations in biological systems.[31-33] One unique advantage of ESI-MS over other techniques is its capability of directly and simultaneously detecting multiple species present in solution, which allows calculation of molecular association stoichiometry based on mass to charge ratio. For multi-component systems, caution needs to be taken when correlating the concentration of individual types of molecules at equilibrium in solution with the relative abundance of corresponding charged ions measured in the gas phase. Previous studies by ESI-MS on concentration-dependent and solvent-dependent nanoaggregation of a synthetic polyaromatic compound (C5Pe) revealed an overall increase in relative abundances of C5Pe nanoaggregates with increasing C5Pe concentration or addition of heptane in solution.[34] Now, ESI-MS technique is applied to studying nanoaggregation of synthetic polyaromatic compounds, individually and in mixtures under various solution conditions. All the ESI-MS tests were conducted using solutions containing 50% methanol and 4mM NH_4Ac by volume to enhance the efficiency of electrospray ionization. The focus was on comparison of overall change in relative abundances instead of the absolute peak intensity values under various solution conditions at a fixed methanol volume fraction.

Figure 2(a) shows the ESI mass spectrum acquired in negative ion mode using 1:1 methanol-in-toluene (M-T) solution containing 10 μM C5PeC11 and 4 mM NH_4Ac. The dominant peaks on the ESI mass spectrum corresponded to C5PeC11 monomer. Only C5PeC11 dimers and trimers were observed at relatively low abundances. This observation is completely different from previous reported results of C5Pe,[34] which at the same solute concentration and solution

condition exhibited much stronger nanoaggregation as $C5Pe_n^{z-}$, where n varied between 7-11, 15 and 17. The results clearly show a lower degree of nanoaggregation by increasing the length of aliphatic chain to introduce steric and/or solubility effects. As anticipated, increasing the concentration of C5PeC11 to 40 µM increased relative abundances of dimer and trimer, accompanied by small peaks corresponding to 5 and 6-mers on the mass spectrum (Figure 2(b)).

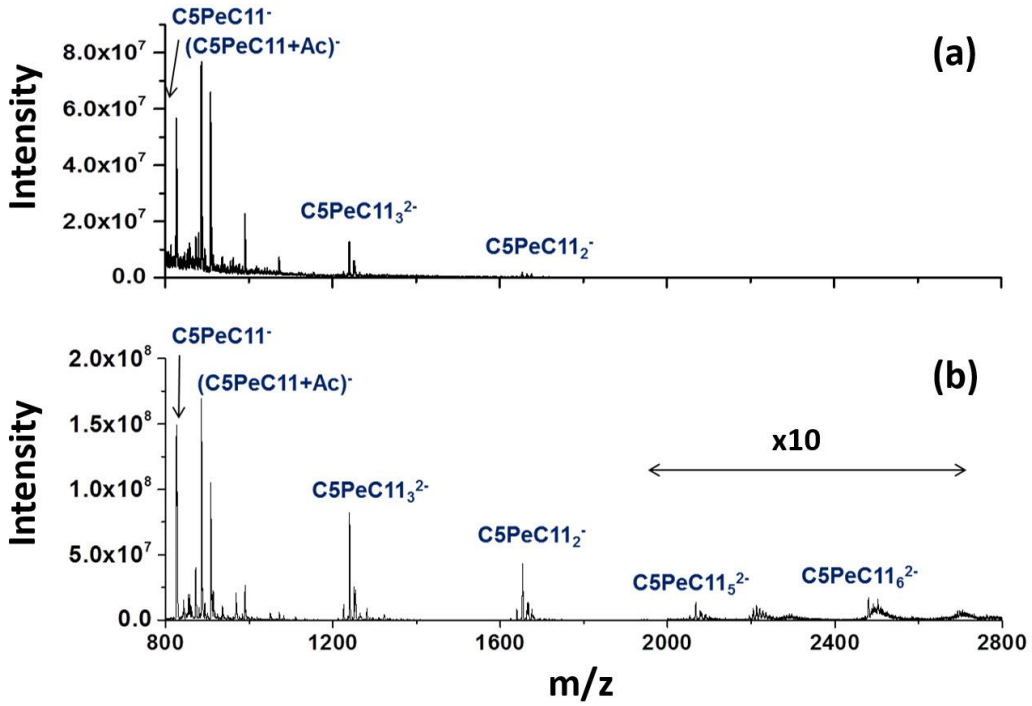

Figure 2. ESI mass spectra acquired for solutions (25 °C) of (a) 10 µM and (b) 40 µM C5PeC11 with 4mM NH_4Ac in 50% methanol and 50% toluene mixture.

To quantify the nanoaggregation, the fraction for each class of C5PeC11 nanoaggregates (including monomer) is calculated as the sum of MS peak intensities of the aggregates at different charge states ($\sum_z Ab(\mathrm{C5PeC11_n^{z-}})$) multiplied by its aggregation number (n), and then divided by the total number of C5PeC11 molecules ($\sum_n(\mathrm{n} \times \sum_z Ab(\mathrm{C5PeC11_n^{z-}}))$) in all the nanoaggregates (eq. 1).

$$f(\%) = \frac{\mathrm{n}\times\sum_z Ab(\mathrm{C5PeC11}_{\mathrm{n}}^{\mathrm{z}-})}{\sum_n(\mathrm{n}\times\sum_z Ab(\mathrm{C5PeC11}_{\mathrm{n}}^{\mathrm{z}-}))} \times 100\% \qquad (1)$$

It should be noted that the reproducibility of ESI-MS measurement is quite good with the standard deviation values of f (%) calculated from four repeating measurements being within ±2%. The results are plotted in Figure 3(a) as the relative abundance distribution of all C5PeC11 nanoaggregates determined by ESI-MS technique performed at the same solution condition (4mM NH_4Ac, 1:1 M-T solution) with varying C5PeC11 concentrations from 10, 20 and 30 to 40 μM.

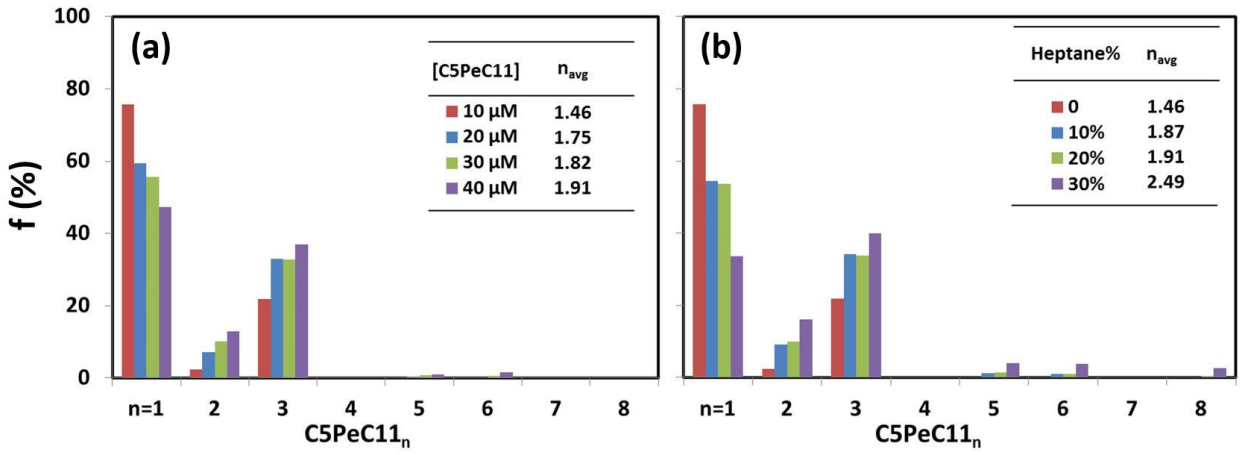

Figure 3. Distribution of relative abundance of C5PeC11 nanoaggregates measured in solutions containing (a) C5PeC11 at 10, 20, 30 and 40 μM, and (b) 10μM C5PeC11 at different volume percentage of heptane, versus aggregation number (n). All the solutions contain 4 mM NH_4Ac and 50% methanol by volume. Volume of toluene is balanced by volume of methanol and heptane. The apparent average nanoaggregation number values (n_{avg}) are shown in the inset.

Figure 3(a) shows that increasing C5PeC11 concentration reduced the relative abundance of C5PeC11 monomers, and increased the fractions of dimers and trimers. Larger nanoaggregates, such as 5-mer and 6-mer were observed but only at very low abundance even at very high C5PeC11 concentrations. Different from much larger nanoaggregates (n≥7) of C5Pe at high

concentrations,[34] the dominant nanoaggregates of C5PeC11 were still limited to dimers and trimers even at 40 μM C5PeC11. The apparent average nanoaggregation number (n_{avg}) is calculated using equation 2:

$$n_{avg} = \sum_n nf\%(\mathrm{C5PeC11}_n) \quad (2)$$

where fraction of each C5PeC11 nanoaggregate, $f\%(\mathrm{C5PeC11}_n)$, is calculated using equation 1. The average nanoaggregation number increased slightly from 1.46 to 1.91 with increasing C5PeC11 concentration from 10 to 40 μM. For C5Pe, a corresponding increase in n_{avg} value from 5.14 to 7.19 is observed when increasing the C5Pe concentration from 10 to 30 μM. It appears that the level of nanoaggregation is much more sensitive to concentration for C5Pe than for C5PeC11.[34]

The effect of heptane addition on nanoaggregation of C5PeC11 was investigated by adding a varying amount of heptane into 10 μM C5PeC11 solutions. The results in Figure 3(b) show that at a constant C5PeC11 concentration, an increase in heptane content from 0 to 30% reduced the monomer fraction of C5PeC11 from 76% to 33%, contrarily to the gradual increase in the fraction of dimer and trimer. Although a very low relative abundance of $\mathrm{C5PeC11}_n$ nanoaggregates with n=5~8 were observed when adding heptane, the dominant nanoaggregation level for C5PeC11 was still dimers and trimers. The calculated n_{avg} value at 30% heptane is 2.49 (Figure 3(b)). This observation differs also from the reported result for C5Pe with shorter aliphatic chain, where $\mathrm{C5Pe}_n$ nanoaggregates with n=2~31 were detected in the mass spectrum with an n_{avg} value around 7 at 30% of heptane.[34] These contrast results indicate that the steric hindrance component with higher solubility due to longer aliphatic chain of C5PeC11 might reduce or further sterically hinder the intermolecular interactions between the C5PeC11 molecules, resulting in a lower level of nanoaggregation.

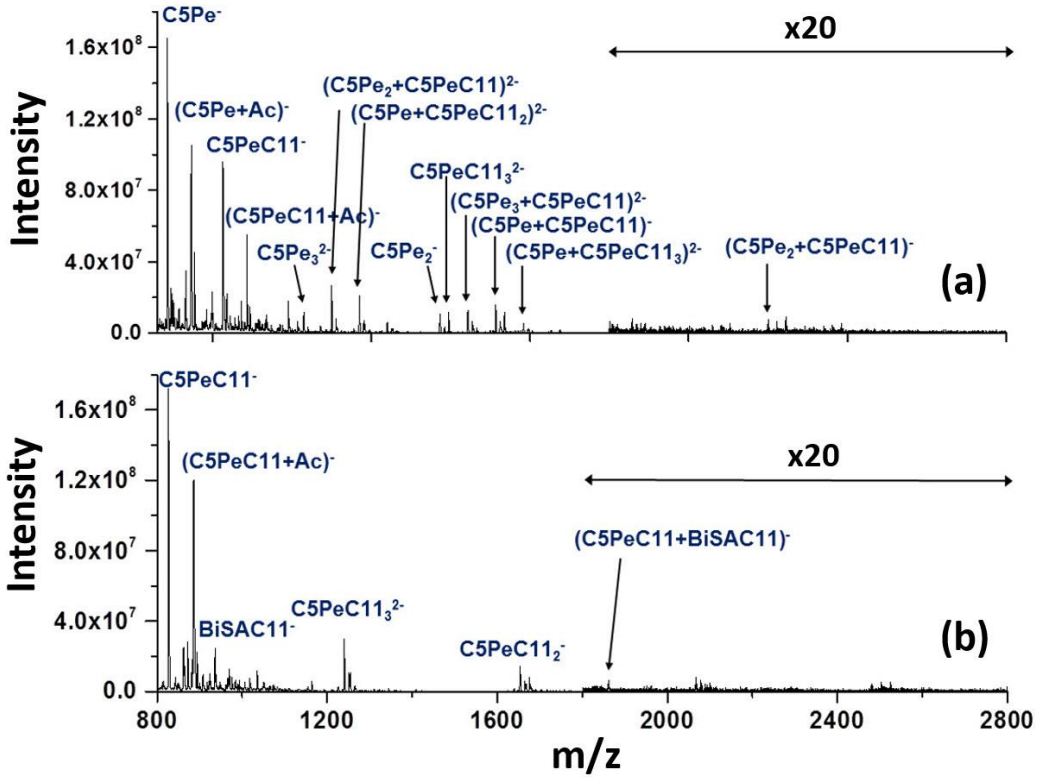

Figure 4. ESI mass spectra acquired for solutions (25 °C) of (a) 10 µM C5PeC11 with 10 µM C5Pe and (b) 40 µM C5PeC11 with 11 µM BisAC11 in 1:1 M-T solutions containing 4mM NH_4Ac.

A major limitation in studying aggregation of asphaltenes using model compounds is the inherent nature of polydispersity of asphaltene molecules as a solubility class, even with extended SARA fraction by emulsions washing or adsorption. The successful synthesis of C5Pe and C5PeC11 made it possible to investigate the influence of the polydispersity on nanoaggregation of asphaltene-like polyaromatic molecules. For this purpose as the main objective of the current study, the nanoaggregation study was extended to the mixtures of C5PeC11 with two other polyaromatic compounds, C5Pe and BisAC11. Figure 4(a) shows the ESI-MS mass spectrum of 1:1 M-T solution containing 10 µM C5PeC11 and 10 µM C5Pe in negative ion mode. Upon mixing of C5PeC11 with C5Pe at 25 ^{o}C, dominant peaks

corresponding to C5Pe and C5PeC11 monomers were observed. Peaks corresponding to nanoaggregates of C5Pe, C5PeC11 and their C5Pe-C5PeC11 complexes are much lower. Shown in Figure 5(a) is the distribution of nanoaggregates plotted as a function of the total nanoaggregation number (n_{total} = n + m) of ($C5Pe_m$+$C5PeC11_n$) in all nanoaggregates. Addition of 5 μM C5PeC11 into 10 μM C5Pe is clearly seen to decrease the aggregation number range from 2 to 19 in pure C5Pe system to that from 2 to 5, despite of the increase in total concentration of polyaromatic molecules in the system from 10 μM to 15 μM. As a result, the calculated n_{avg} value decreased from 5.14 in C5Pe to 1.87 with the addition of 5 μM C5PeC11. No significant decrease in n_{avg} value was observed when the concentration of C5PeC11 was further increased to 20 μM, which was due to the absence of $C5PeC11_n$ nanoaggregates with n > 5. At this concentration level (20 μM), replacing 10 μM C5PeC11 with 10 μM C5Pe did not change the relative population of C5PeC11 nanoaggregates as compared with the distribution for C5PeC11 alone. The average aggregation number is slightly higher in the presence (1.94) than in the absence (1.75) of C5Pe, but significantly lower than the value for corresponding 20 μM C5Pe solutions (5.27).[34] It seems like C5PeC11 is able to increase the solubility of C5Pe and disperse it under these solution conditions. An increase in the aliphatic chain length by five methylene units in C5PeC11 seems to induce extra steric component to reduce the intermolecular interactions (mainly π-π stacking, polar group interactions and hydrogen bond) between C5PeC11 molecules and among C5Pe, resulting in limited nanoaggregation and preventing formation of larger nanoaggregates.

In order to investigate the effect of polarity on the nanoaggregation of polyaromatic compounds, nanoaggregation of C5PeC11 and BisAC11 mixture was investigated. In contrast to C5PeC11, BisAC11 has the same aliphatic chain on both ends of the molecule without a terminal

carboxylic group (Figure 1). As shown in the ESI mass spectrum (Figure 4(b)), the dominant peaks for single C5PeC11 system did not change when BisAC11 was added (Figure 2(b)). The peaks mainly correspond to C5PeC11 monomer, although weak peaks corresponding to a 1:1 $(C5PeC11:BisAC11)^-$ complex were noticeable on the mass spectrum. Interestingly only a small peak representing BisAC11 monomer was observed, mainly due to low electrospray ionization efficiency at negative ion mode for the nonpolar BisAC11.

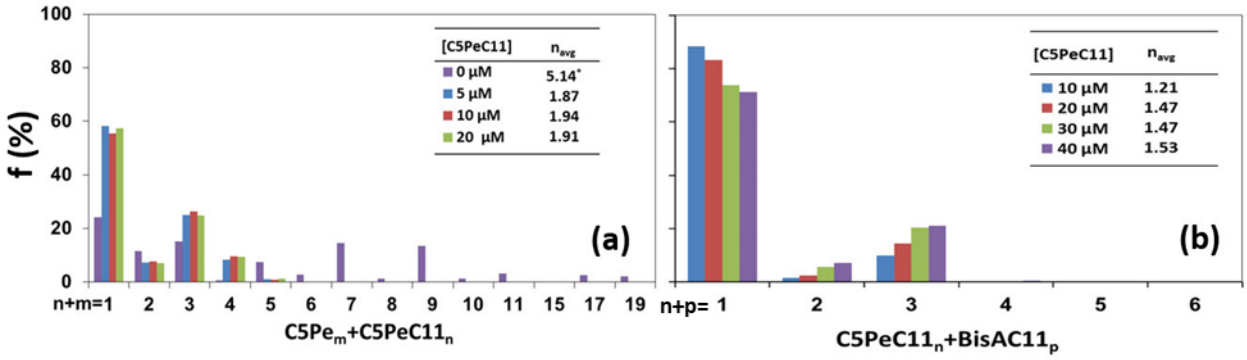

Figure 5. Distribution of relative abundance of nanoaggregates versus total aggregation number (n_{total}) in polyaromatic compound solutions of (a) 10 µM C5Pe with 0, 5, 10 and 20 µM C5PeC11, and (b) 10 µM BisAC11 with 10, 20 30 and 40 µM C5PeC11 in 50:50 (v/v) methanol:toluene (M-T) solutions containing 4mM NH_4Ac. The data for solution containing 10 µM C5Pe (*) is from reference 34.

Displayed in Figure 5(b) are the relative populations of nanoaggregates as a function of total aggregation number in C5PeC1-BisAC11 mixture. The fraction of C5PeC11 and BisAC11 monomers decreased, while the fraction of small nanoaggregates increased gradually with increasing C5PeC11 concentration. It is interesting to note that in the presence of 10 µM BisAC11, the fraction values of monomers are consistently higher and the fraction values of nanoaggregates are consistently lower than the corresponding case of C5PeC11 without BisAC11 (Figure 3(a)). It can be seen clearly from n_{avg} values that at the same C5PeC11

concentration, the average aggregation number in the presence of BisAC11 is systematically lower than that in the absence of BisAC11, i.e., the self-association of C5PeC11 was further reduced in the presence of BisAC11. This result is consistent with the observations from isothermal titration calorimetry (ITC) measurement on C5PeC11-BisAC11 mixtures, where the solubility of C5PeC11 was shown to increase upon addition of BisAC11 due to a 1:1 complexation between C5PeC11 and BisAC11 molecules.[35] These results collectively suggest that a lower polarity achieved by replacing the -COOH group with a double aliphatic chain will further increase the steric hindrance and preventing the nanoaggregation.

To study the tolerance of nanoaggregation in multi-component systems to the quality of solvent, normal heptane was added to the mixture of polyaromatic compounds. Figure 6 shows the variations in relative abundance of nanoaggregates in solutions of higher normal heptane content. For C5Pe-C5PeC11 mixtures, adding 30% heptane decreased only slightly the relative abundance of monomers, accompanied by a small increase in fraction of nanoaggregates at low aggregation numbers (n=2~6). Under these solution conditions, the n_{avg} value showed a considerable change from 5.14 to 7.42 with 30% heptane addition to a pure 10 μM C5Pe in toluene solution.[34] The corresponding n_{avg} values in C5Pe-C5PeC11 mixtures (10 μM C5PeC11+10 μM C5Pe) increased only slightly from 1.94 (in the absence of heptane) to 2.27 at 30% of heptane. The results show a higher tolerance of nanoaggregation to the addition of heptane in C5Pe-C5PeC11 mixtures. Similar results were observed in C5PeC11-BisAC11 mixture systems where the n_{avg} value increased from 1.21 to 1.62 with 30% heptane addition. Figure 3(b) displays the effect of increasing heptane content from 0 to 30% on C5PeC11 aggregation in 10 μM solution without BisAC11, showing an increase in n_{avg} value from 1.46 to 2.49.

In summary, all the results show that an increase in the length of aliphatic chain connected to the polyaromatic core can effectively disperse the perylene bisimides-based compounds and reduce the nanoaggregation. For the three asphaltene-like polyaromatic compounds, the observed aggregation trend of BisAC11 < C5PeC11 < C5Pe is in line with their decreased solubility in aromatic solvents.

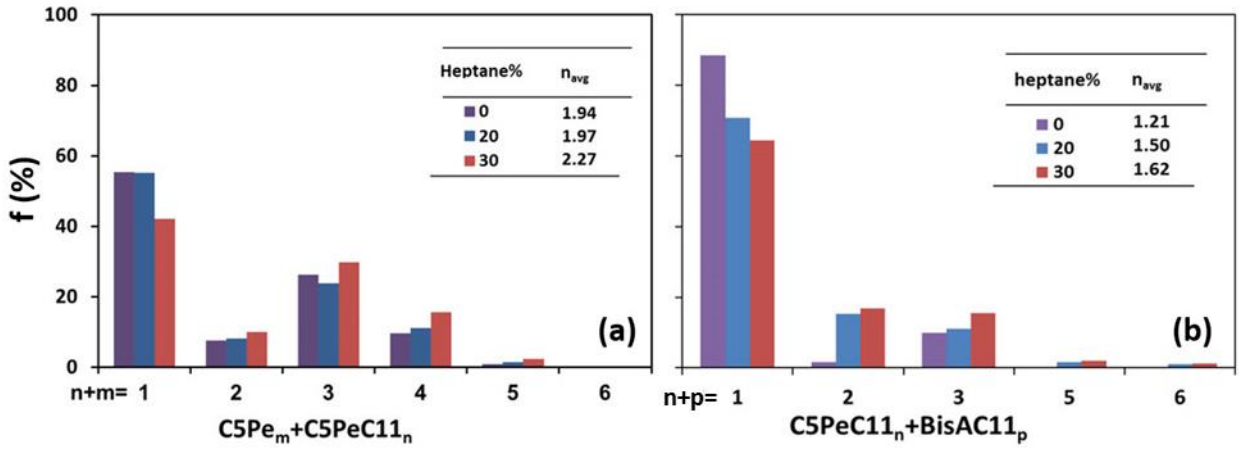

Figure 6. Distribution of relative abundance of nanoaggregates measured in binary polyaromatic compound solutions at various heptane additions versus total aggregation number (n_{total}). Binary polyaromatic compound solution contains (a) C5Pe 10 µM and C5PeC11 10 µM, and (b) BisAC11 10 µM and C5PeC11 10 µM.

Molecular dynamics simulation on nanoaggregation

In order to identify possible intermolecular interactions responsible for the observed nanoaggregation, MD simulations were performed on three individual polyaromatic compounds and their mixtures in 1:1 methanol-toluene (M-T) mixtures. The M-T mixture was studied by MD simulations as methanol was added in ESI-MS experiments to enhance ionization of molecules/aggregates for detection by ESI-MS. Demonstration of achieving dynamic equilibrium using quantities such as the radial distribution functions (RDFs) for the center of mass (COM) of

polyaromatic cores and velocity autocorrelation function (VACF) of polyaromatic molecules generated using the last 1 ns of the simulation time are available in the Supporting Information (see Supporting Information S3-S4). The definition for core group of polyaromatic molecules were given in Supporting Information S2). Figure 7 shows the radial distribution functions (RDFs) for the COM of polyaromatic cores away from a reference polyaromatic molecule, g(r). These RDFs are the average over the last 2 ns of a total of 30 ns simulation. For all the systems in 1:1 M-T, three peaks were seen at the core-to-core distance of 0.36, 0.72 and 1.09 nm. Irrespective of the nature of the polyaromatic molecules, the positions of these three peaks are almost identical for all the polyaromatic molecules. The first and the most prominent peak is located at ~0.36 nm in all the cases. This value agrees well with the reported distance of ~0.35 nm between π-π stacked polyaromatic cores, indicating the formation of strong π-π stacking between polyaromatic cores within nanoaggregates.[36] For three pure polyaromatic compounds in 1:1 M-T, the intensity of the first peak in the RDF follows the order of C5Pe > C5PeC11 > BisAC11 (Figure 7(a)). The progressive reduction in the peak height from C5Pe to C5PeC11 and BisAC11 indicates the reduced number of direct π-π stacking from BisAC11 to C5PeC11 and C5Pe, most likely as a result of the increased steric hindrance due to increasing aliphatic chain length and reduced polarity from C5Pe to C5PeC11 and BisAC11 in 1:1 M-T mixture. These results agree well with the results from the ESI-MS experiments which showed stronger nanoaggregation of C5Pe than C5PeC11 followed by BisAC11. It is interesting to note the distance of 0.36 nm between the first and second peaks and 0.37 nm between the second and third peaks in RDFs, suggesting an extended π-π stacking of the molecules to the second and third layers with the third layer being slightly diffused or less ordered. The nearly identical spacing between the neiboughering peaks of the RDFs suggests π-π stacking being the main

driving force for nanoaggregation of these three polyaromatic compounds in 1:1 M-T mixture although to less extent for BisAC11.

When mixed with C5PeC11, Figure 7(b) shows a significant decrease in the intensity of the first peak in RDF as compared with the case of C5Pe alone. This finding clearly suggests a dispersive role of C5PeC11 in C5Pe nanoaggregation: the addition of C5PeC11 into C5Pe severely depressed the π-π stacking between C5Pe molecules. Similar result can be observed for the addition of BisAC11 into C5PeC11 (Figure 7(c)), with a much lower intensity of the first peak in RDF of 24 C5PeC11 in 24 BisAC11 + 24 C5PeC11 than in pure 24 C5PeC11 system. This result indicates that the intermolecular interactions (π-π stacking and hydrogen bond) stabilizing C5PeC11 nanoaggregates can be further hindered by introducing dispersant molecules (BisAC11) with reduced polarity and longer side chains. All these results further confirm the strongest dispersing capability of BisAC11 within the three polyaromatic compounds. Thus, C5PeC11 can be used to disperse and reduce the nanoaggregation of C5Pe, while BisAC11 with the least aggregation tendency can be used to further supress nanoaggregation of C5PeC11. All the trends observed from MD simulation are in an excellent agreement with those observed in ESI-MS experiments (see Figure 5). It should be noted that the quantitative comparison of the results between ESI-MS and MD simulation is not possible as the result of much higher concentrations of polyaromatic molecules in MD simulations than in ESI-MS experiments, limited by representative systems of 24 (single species) or 48 (mixtures) molecules with around 13000 solvent molecules. To simulate the system concentration of ESI-MS experiments with similar 24 and 48 polyaromatic molecules would need 2.8×10^{10} and 3.1×10^{10} solvent molecules, respectively, to contrast simulation system that would not be possible with current computing facility.

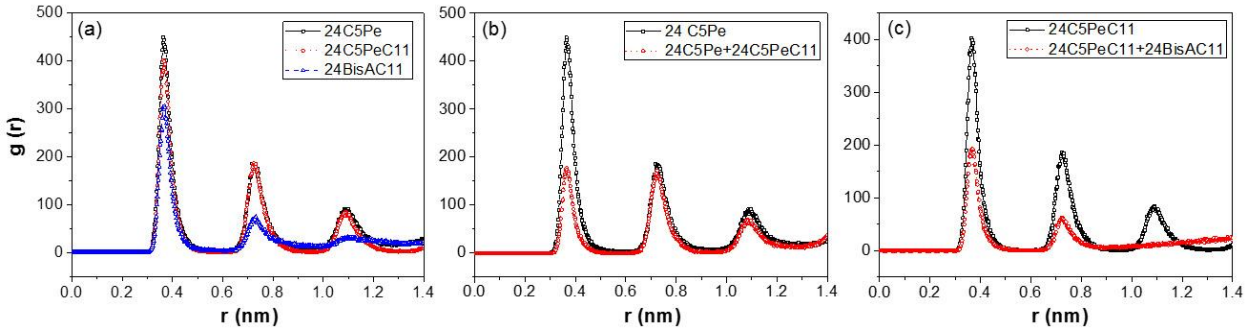

Figure 7. Radial distribution functions for the COM separation distance r (nm) between aromatic cores over the last 2 ns for 30 ns of simulations. (a) 24 C5Pe, 24 C5PeC11, and 24 BisAC11 in 1:1 M-T; (b) 24 C5Pe alone or 24 C5Pe in binary system with 24 C5PeC11 in 1:1 M-T; and (c) 24 C5PeC11 alone or 24 C5PeC11 in binary system with 24 BisAC11 in 1:1 M-T.

To probe the state of molecular aggregation, snapshots of the simulation box at t = 30 ns for each of three polyaromatic molecules are shown in Figure 8(a-c). From these snapshots we can directly observe that all three individual polyaromatic molecules form nanoaggregates to varying degrees of association. Among the three systems, BisAC11 as in Figure 8(c) shows the least aggregation without clear π-π stacking between polyaromatic cores in the snapshot view, mainly due to the reduced polarity and steric hindrance resulting from four long hydrocarbon side chains attached to the polyaromatic core. The four long hydrocarbon chains on BisAC11 tend to tangle together and block the close approach of polyaromatic cores to prevent the formation of π-π stacking. In contrast, tetramers is clearly seen in 24 C5Pe molecules as shown in Figure 8(a), while the largest nanoaggregates in 24 C5PeC11 molecules is trimers as shown in Figure 8(b). In addition, there are more monomers in C5PeC11 system than in C5Pe system as shown in Figure 8(b). This observation supports the experimental results that the relative abundance of monomers in C5PeC11 system was higher than that in C5Pe system. The increased chain length for C5PeC11 introduces larger steric hindrance for nanoaggregation and results in an increase in the

solubility of C5PeC11. The dispersion of C5Pe by higher solubility C5PeC11 is clearly seen in Figure 8(d), where a significant increase in association of C5PeC11 with C5Pe as dimers at the cost of higher degree of associations was observed. Such association of C5PeC11 molecules with C5Pe induced steric hindrance, preventing self-association of C5Pe molecules into larger nanoaggregates. Similarly, the addition of BisAC11 was able to further disperse C5PeC11 substantially as shown in Figure 8(e), due mostly to strong association of more soluble BisAC11 with C5PeC11 of similar aliphatic tail length.

To confirm the increased solubility or solvation of C5PeC11 than C5Pe, MD simulation results were analyzed to determine the solvent-accessible surface area (SASA) defined as the area of a polyaromatic molecule in contact with solvent molecules. A higher SASA value indicates a more solvated state of the polyaromatic molecules, translating to an increased solubility of the molecules, which is an important factor accounting for less aggregation. The results in Figure 9(a) show an increased SASA value in the order of BisAC11 > C5PeC11 > C5Pe. Combing this order of solvation with larger steric hindrance resulting from long side chains, one would expect an increased extent of nanoaggregation from BisAC11 to C5PeC11 and then to C5Pe. The observed trend in MD simulation agrees well with the results from ESI-MS experiments and provides theoretical insights for studying mechanisms of nanoaggregation of polyaromatic compounds in organic solvents.

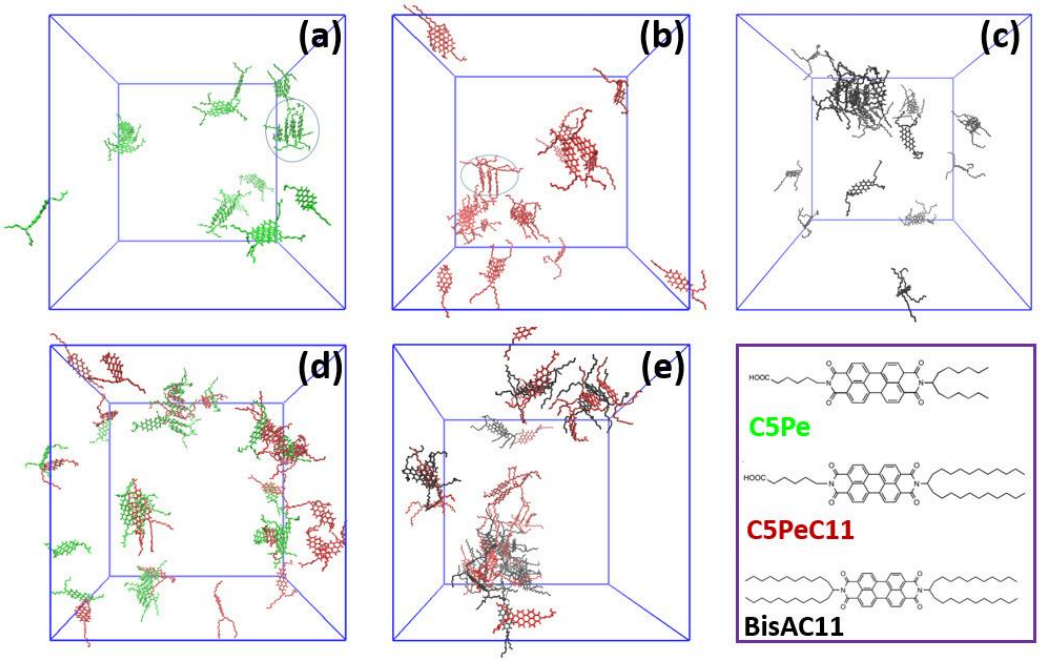

Figure 8. Snapshots of polyaromatic molecules in 1:1 M-T, taken at the end of 30 ns simulation time. Each molecule is presented by a different color to distinguish one from the other: C5Pe in green, C5PeC11 in red, and BisAC11 in black. Solvent molecules are removed for clarity. (a) 24 C5Pe in 1:1 M-T; (b) 24 C5PeC11 in 1:1 M-T; (c) 24 BisAC11 in 1:1 M-T; (d) 24 C5Pe + 24 C5PeC11 in 1:1 M-T; (e) 24 BisAC11 + 24 C5PeC11 in 1:1 M-T. Tetramers formed by C5Pe and trimers formed by C5PeC11 were circled in the snapshot for clarity.

Compared with the single C5Pe system, the addition of C5PeC11 significantly increased SASA as shown in Figure 9(b). In fact, the SASA value of C5Pe in 24 C5Pe + 24 C5PeC11 system is very close to the value of C5PeC11 single component system, indicating increased accessibility of C5Pe molecules by solvent molecules due to the presence of C5PeC11. This observation confirmed that the addition of C5PeC11 is beneficial for reducing nanoaggregation of C5Pe and increased solubility of C5Pe. Similarly, adding BisAC11 of less aggregation tendency and higher solubility could disperse C5PeC11 and increase its solubility, shown in Figure 9(c) as a significant increase in SASA value of C5PeC11 in the binary system as compared with single

C5PeC11 system. The results above collectively confirm that the increased steric hindrance from the increased chain length and reduced polarity by replacing -COOH with double aliphatic chain can effectively hinder the formation of large aggregates.

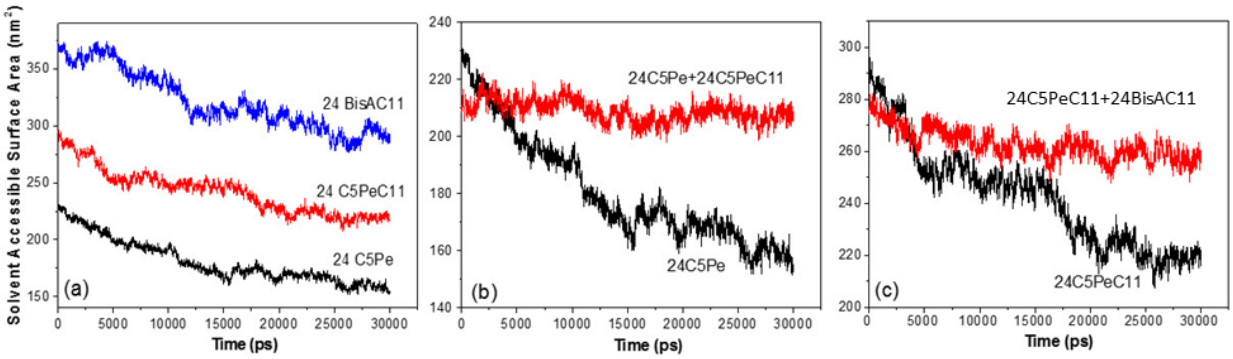

Figure 9. Solvent-accessible surface area of the polyaromatic molecules over the simulation time for (a) 24 single component molecules in 1:1 M-T; (b) 24 C5Pe alone or 24 C5Pe in binary system with 24 C5PeC11 in 1:1 M-T; (c) 24 C5PeC11 alone or 24 C5PeC11 in binary system with 24 BisAC11in 1:1 M-T.

The snapshots give us a general idea that C5PeC11 molecules were able to insert between C5Pe to act as disperse agent as shown in Figure 8(d). In order to quantify the dispersing effect of C5PeC11 on aggregation of C5Pe molecules, we further analyzed mode of molecular stacking as m-MS where m represents the number of C5Pe molecules directly associated into a single nanoaggregate. For example, if the COM distance between molecules 1 and 2, and 2 and 3 are both less than 0.44 nm, then molecules 1, 2 and 3 are said to form three-molecule stacking, i.e., 3-MS. The COM distances between molecules were averaged over the last 2 ns of the simulation time. The m calculated for 24 C5Pe in single species system and in binary system with 24 C5PeC11 molecules is shown in Table 2. The results indicate an effective depression on C5Pe aggregation by C5PeC11 addition as shown by a reduction in 4-MS from 4 to 1, although the overall size of aggregates formed by C5Pe and C5PeC11 in solutions of higher overall

concentration (24 C5Pe and 24 C5PeC11) is larger than that in lower concentration solutions of 24 C5Pe alone. Similar dispersion effect of BisAC11 on C5PeC11 aggregation is also observed. As shown in Table 2, the number of C5PeC11 trimers decreased from 5 to 1, accompanied by an increase in the number of C5PeC11 dimers as a result of increased solubility, larger steric hindrance and reduced polarity provided by BisAC11. The results of MD simulation agree well with the experimental results of ESI-MS experiments and clearly suggest that polyaromatic molecules of less aggregation tendency and higher solubility could be used as a dispersing agent to hinder the aggregation of higher aggregation tendency and lower solubility polyaromatic molecules.

Table 2. Number of m-MS C5Pe aggregates formed from 24 C5Pe alone or 24 C5Pe in binary system with 24 C5PeC11 in 1:1 M-T, and m-MS C5PeC11 aggregates formed from 24 C5PeC11 alone or 24 C5PeC11 in binary system with 24 BisAC11 in 1:1 M-T.

Aggregate type	4-MS	3-MS	2-MS
24 C5Pe	4	0	3
24 C5Pe with 24 C5PeC11	1	0	3
24 C5PeC11	0	5	1
24 C5PeC11 with 24 BisAC11	0	1	4

Conclusions

The results of electrospray ionization-mass spectrometry (ESI-MS) experiments at a given concentration of single component polyaromatic molecules in 1:1 (v/v) methanol-toluene (M-T) solution showed the highest average nanoaggregation number of C5Pe, followed by C5PeC11 and then BisAC11, indicating a higher aggregation tendency of polyaromatic molecules of shorter aliphatic chains and/or containing -COOH groups. The addition of polyaromatic

compounds of longer aliphatic chains significantly reduced the overall average nanoaggregation number of the binary mixture in 1:1 M-T solutions. Replacing the -COOH group with another aliphatic chain in the binary mixture resulted in further steric hindrance to nanoaggregation in 1:1 M-T solutions. Although the addition of heptane or increasing concentration of polyaromatic compounds enhanced nanoaggregation of single component polyaromatic molecules, adding other polyaromatic compounds of less self-association tendency counter-balanced the observed enhancement by increased overall concentration of polyaromatic molecules and heptane addition. The nanoaggregation tendency of polyaromatic compounds observed in ESI-MS experiments was confirmed by the results of MD simulations. MD simulation provided scientific insights of observed difference in nanoaggregation of different polyaromatic molecules as a result of steric hindrance, despite their similar aggregation mechanisms of π-π stacking. Solubility of polyaromatic molecules in the solvent is a critical factor to determine self-association of corresponding polyaromatic molecules. Longer aliphatic chain and reduced polarity of a given polyaromatic compound were shown to increase its solubility as shown by increased solvation, leading to less aggregation. Adding other compounds of less self-association tendency reduced the degree of nanoaggregation, exhibiting dispersion effect of the polyaromatic molecules with the increase in solvation of the self-associating polyaromatic molecules.

Acknowledgements

This research was conducted under the auspices of the Natural Sciences and Engineering Research Council (NSERC)-Industrial Research Chair (IRC) Program in Oil Sands Engineering. The partial support from Alberta Innovates - Energy and Environmental Solutions is also greatly appreciated. The authors thank JIP Asphaltene consortium “Improved Mechanism of Asphaltene

Deposition, Precipitation and Fouling to Minimize Irregularities in Production and Transport – A Cost Effective and Environmentally Friendly Approach funded by Norwegian Research Council (NFR PETROMAKS, Grant number - 234112)", consisting of Ugelstad Laboratory (NTNU, Norway), University of Alberta (Canada), University of Pau (France) and Federal University of Paraná (Brazil) with following industrial sponsors - AkzoNobel, BP, Canada Natural Resources, Nalco Champion, Petrobras, Statoil and Total. Rongya Zhang acknowledges financial support from Tianjin University and China Scholarship Council (CSC). We also acknowledge computing resources and technical support from Western Canada Research Grid (Westgrid).

References

1. Hao, L.; Jia, Y.; Liu, Q.; Wang, Y.; Xu, G.; Nan, Y. *Colloids and Surfaces A: Physicochem. Eng. Aspects* **2016**, *511*, 91-104.
2. Alam, M. S; Ragupathy, R.; Mandal, A. B. *J. Disper. Sci. Tech.* **2016**, *37*, 1645-1654.
3. Sinha, S.; Tikariha, D.; Lakra, J.; Tiwari, A. K.; Saha, S. K.; Ghosh, K. K. *J. Surfact. Deterg.* **2015**, *18*, 629-640.
4. Das. S.; Mondal, S.; Ghosh, S. *J. Chem. Eng. Data* **2013**, *58*, 2586-2595.
5. Naorem, H.; Devi, S. *J. Surface Sci. Technol*. **2006**, *22*, 89-100.
6. Akbarzadeh, K.; Bressler, D. C.; Wang, J.; Gawrys, K. L.; Gray, M. R.; Kilpatrick, P. K.; Yarranton, H. W., *Energy & Fuels* **2005,** *19*, 1268-1271.
7. Rakotondradany, F.; Fenniri, H.; Rahimi, P.; Gawrys, K. L.; Kilpatrick, P. K.; Gray, M. R., *Energy & Fuels* **2006,** *20*, 2439-2447.
8. Tan, X.; Fenniri, H.; Gray, M. R., *Energy & Fuels* **2007**, *22*, 715-720.
9. Nordgård, E. L.; Landsem, E.; Sjöblom, J., *Langmuir* **2008**, *24*, 8742-8751.
10. Wei, D.; Orlandi, E.; Barriet, M.; Simon, S.; Sjöblom, J. *J Therm. Anal. Calorim.* **2015**, *122*, 463-471.

11. Teklebrhan, R. B.; Ge, L.; Bhattacharjee, S.; Xu, Z.; Sjöblom, J., *J. Phys. Chem. B*, **2012**, *116*, 5907-5918.

12. Teklebrhan, R. B.; Jian, C.; Choi, P.; Xu, Z.; Sjoblom, J., *J. Phys. Chem. B*, **2016**, *120*, 3516-3526.

13. Teklebrhan, R. B.; Ge, L.; Bhattacharjee, S.; Xu, Z.; Sjöblom, J., *J. Phys. Chem. B*, **2014**, *118*, 1040-1051.

14. Jian C, Tang T, Bhattacharjee S. *Energy & Fuels* **2013**, *27*, 2057-2067.

15. Berendsen, H. J.; van der Spoel, D.; van Drunen, R., *Comput. Phys. Comm.* **1995**, *91*, 43-56.

16. Lindahl, E.; Hess, B.; Van Der Spoel, D., J. Mol. Moldel. **2001**, *7*, 306-317.

17. Oostenbrink, C.; Villa, A.; Mark, A. E.; Van Gunsteren, W. F., *J. Comput. Chem.* **2004**, *25*, 1656-1676.

18. Van Der Spoel, D.; Lindahl, E.; Hess, B.; Groenhof, G.; Mark, A. E.; Berendsen, H. J., *J. Comput. Chem.* **2005**, *26*, 1701-1718.

19. Canzar, S.; El-Kebir, M.; Pool, R.; Elbassioni, K.; Malde, A. K.; Mark, A. E.; Geerke, D. P.; Stougie, L.; Klau, G. W., *J. Comp. Biol*. **2013**, *20*, 188-198.

20. Koziara, K. B.; Stroet, M.; Malde, A. K.; Mark, A. E., *J. Chemput. Aided Mol. Des.* **2014**, *28*, 221-233.

21. Malde, A. K.; Zuo, L.; Breeze, M.; Stroet, M.; Poger, D.; Nair, P. C.; Oostenbrink, C.; Mark, A. E., *J. Chem. Theory Comput.* **2011**, *7*, 4026-4037.

22. Kuznicki, T.; Masliyah, J. H.; Bhattacharjee, S., *Energy & Fuels* **2008**, *22*, 2379-2389.

23. Kuznicki, T.; Masliyah, J. H.; Bhattacharjee, S., *Energy & Fuels* 2009, *23*, 5027-5035.

24. Hoover, W. G., *Phys. Rev. A.* **1985**, *31*, 1695.

25. Parrinello, M.; Rahman, A., *J. Appl. Phys.* **1981**, *52*, 7182-7190.

26. Berendsen, H. J.; Postma, J. v.; van Gunsteren, W. F.; DiNola, A.; Haak, J., *J. Chem. Phys.* **1984**, *81*, 3684-3690.

27. Verlet, L., Computer" experiments" on classical fluids. I. *Phys. Rev.* **1967**, *159*, 98.

28. Essmann, U.; Perera, L.; Berkowitz, M. L.; Darden, T.; Lee, H.; Pedersen, L. G., *J. Chem. Phys.* **1995**, *103*, 8577-8593.

29. Hess, B., *J. Chem. Theory Comput.* **2008**, *4*, 116-122.

30. Humphrey, W.; Dalke, A.; Schulten, K., *J. Mol. Graph. Model.* **1996**, *14*, 33-38.

31. Ganem, B.; Li, Y. T.; Henion, J. D. *J. Am. Chem. Soc.* **1991**, *113*, 7818.

32. Kitova, E.; El-Hawiet, A.; Schnier, P.; Klassen, J. *J. Am. Soc. Mass. Spectrom.* **2012**, *23*, 431-441.

33. Liu, L.; Bai, Y.; Sun, N.; Xia, L.; Lowary, T. L.; Klassen, J. S. *Chem. Eur. J.* **2012**, *18*, 12059-12067.

34. Liu, L.; Sjöblom, J.; Xu, Z. *Energy & Fuels* **2016**, *30*, 3742-3751.

35. Simon, S.; Wei, D.; Barriet, M.; Sjöblom, J. *Colloids and Surfaces A: Physicochem. Eng. Aspects* **2016**, *494*, 108-115.

36. Pisula, W.; Tomovic, Z. e.; Simpson, C.; Kastler, M.; Pakula, T.; Müllen, K., Chem. Mater. **2005**, *17*, 4296-4303.

37. Jana, B.; Pal, S.; Bagchi, B., *J. Chem. Sci.* **2012**, *124*, 317-325.